

Lift Off and Breakage of the Structure of Fractal-Like Aggregates

Łukasz Żywczyk^a, Arkadiusz Moskal^b, Rafał Przekop^b

^aPolish Academy of Sciences, Institute of Fundamental Technological Research, ul. Pawińskiego 5B, 02-106 Warsaw, Poland

^bWarsaw University of Technology, Faculty of Chemical and Process Engineering, ul. Waryńskiego 1, 00-645 Warsaw, Poland

rafal.przekop@pw.edu.pl

A new mathematical model of aggregate of N identical spherical particles is proposed. Model is able to simulate aggregates with different flexibility. Mutual forces in normal direction between primary particles are described by spring-mass system with parameters related to the material properties. The flexibility of aggregate structure is controlled by harmonic interaction functions. Developed model was used to study the lift-off phenomenon of aggregates in the fluid. Simulation were performed for numerically generated few population of fractal-like aggregates by Diffusion Limited Aggregation algorithm (DLA), which differ with number of primary particles in aggregate's structure and fractal dimension. Numerical results show that aggregates with more open morphology with fractal dimension in the range of $D_f = 1.6 - 1.8$ are lifted-off easier, compared to aggregates with compacted structure. The effectiveness of the lift off is enhanced by the deformation of the aggregate caused by the flexibility of its structure.

1. Introduction

The lift-off phenomenon is a subject of a special importance in the medical applications such as drug inhalation, where powder structure needs to be reemitted or lifted-off into the flow (Telko and Hickey, 2005) and then broken-up onto the single particles in the air (Gac et al., 2008), in order to deliver effectively active medical substance absorbed on the surface of the medium into the target organ. Most of those transport media are formed in a large easily dispersed agglomerated structures which are composed of many smaller components called primary particles (Brasil et al., 2001).

One of the main issues which is encountered in this field of dynamics of complex aggregates is the description of lift-off phenomenon from the surface and further dynamic behaviour of structure in the air. There are many literature positions regarding the re-entrainment of single particles from the flat surface (Reeks et al., 1988). Such particle located initially on the rigid surface can experience three initial types of movement; rolling, sliding and lift-off, when subjected to the external flow (Gradoń, 2009). Popular well known algorithms like Rock'n'Roll (Reeks and Hall, 2001) describing the resuspension of the particle from the rough surface, can only be applied to the single particle. However, the dynamic behaviour of the complex aggregate structure is very different than the movement of the single particle. Examples of studies regarding the set of N connected identical spherical particles reemitted to the air were analyzed by Grzybowski and Gradoń (2005) who used the oscillatory model to investigate the phenomenon. Gac et al. (2008) used the same approach to derive the energy from turbulent flow, which is required to break-up the bonds between constitutive particles in powder structure. Therefore, one should opt to use the model of aggregate which include modification of the structure under different external factors.

In this study a new model of fractal-like aggregate is presented which is used to demonstrate numerically the lift-off phenomenon of the aggregates which can undergo deformation during their movement in the fluid. We consider a scenario where whole aggregate is lifted and no detachment of the constitutive particles occurs during the process. The investigation conducted here is restricted to the aggregates with unbreakable bonds. However, it would be easy to apply breakage of the bonds.

Paper Received: 18 March 2018; Revised: 4 July 2018; Accepted: 17 December 2018

Please cite this article as: Żywczyk Ł., Moskal A., Przekop R., 2019, Lift Off and Breakage of the Structure of Fractal - Like Aggregate, Chemical Engineering Transactions, 74, 457-462 DOI:10.3303/CET1974077

2. Mathematical model

In the present work, a harmonic oscillator model, defined as a spring – damping system was used to describe the interactions between the connected primary particles in the aggregate, Equation (1). Originally, the model was used to study the re-entrainment of particles from the surface (Reeks et al., 1988). Equation (1) includes both attractive and repulsive forces acting in the normal direction between the connected particles.

$$m_{pi} \frac{d^2 r_i}{dt^2} = -k_s (r_{ij} - r_{0ij}) - f_d \frac{dr}{dt} \quad (1)$$

where m_i is the mass of the particle, t is time, k_s is the bond constant, f_d is the damping factor, r_{ij} is the distance between the geometrical centres of the joined particles, and r_{0ij} is the initial distance between the geometrical centres of the joined particles. The bond constant k_s can be obtained from equation derived by Ziskind et al. (2000):

$$k_s = 2.4 \left(\gamma \kappa^2 \frac{d_p^2}{4} \right)^{1/3} \quad (2)$$

where γ represents the surface energy between the joined particles and d_p is the diameter of the primary particles. The elastic constant κ , which represents the material properties in Equation (2) can be calculated from the formula for two non-identical connected materials:

$$\kappa = \frac{4}{3} \left(\frac{1-\nu_1^2}{E_1} + \frac{1-\nu_2^2}{E_2} \right)^{-1} \quad (3)$$

where E is the Young's modulus and ν is Poisson's ratio. The damping factor f_d is defined as the resistance of the particle-particle mechanical interaction and can be obtained from (Przekop et al., 2004):

$$f_d = \frac{2.4}{\pi} \frac{m_p \kappa^2}{\rho_p \left(\frac{E}{\rho_p} \right)^{3/2}} \quad (4)$$

where ρ_p is particle density. Equation (1) describes only forces which acts in normal direction between geometrical centres of connected constituent primary particles in aggregate. Therefore, the simple harmonic oscillator model, defined as the spring – damping system, was extended. We develop a model where we do not focus only on the forces between immediate joined primary particles, but in addition we use internal forces which control flexibility of the whole aggregate structure. In order to maintain flexibility, there is a need to distinguish subsequent configurations of particles, as illustrated schematically in Figure 1. The interactions in those configurations are described mathematically by different potential energy functions, which will control the resistance of aggregate's structure to deformation. First, we can introduce configurations of particles in the model of a flexible fractal-like aggregate:

a) Pairs of bonded particles $i-j$, Figure 1 (a), described by the harmonic bond potential energy function, Equation (5); b) Triplets of particles $i-j-k$ and two pairs of bonded particles, $i-j$ and $k-j$, connected via one common particle j , Figure 1 (b), described by the harmonic cosine angle potential energy function, Equation (6); c) Quadruple of particles $i-j-k-l$ and two pairs of bonded particles, $i-j$ and $l-k$, connected via a middle pair $j-k$, Figure 1 (c), described by the torsion potential energy function, Equation (9); d) Quadruple of particles $i-j-k-l$ and triplet of particles $i-j-k$ connected with the last particle l via a bond with the middle particle j , Figure 1 (d), described by the inversion potential energy function.

Functions that describe the interactions between particles in the above-mentioned configurations are represented by four potential energy functions, which will be described below. Primary interaction which govern the interaction forces in normal direction between connected particles is mathematical described by the force derived from Equation (5). This interaction keeps the distance between the geometrical centres of connected particles $i-j$ close to the value of r_{0ij} :

$$V_a(r_{ij}) = \frac{1}{2} k_s (r_{ij} - r_{0ij})^2 \quad (5)$$

Equation (5) was differentiated to provide the internal force acting on the primary particles.

For the primary particles set up in configuration depicted on Figure 1 (b), the harmonic cosine angle potential energy function, Equation (6) was applied. Equation (6) keeps the angle between the pairs of particles $i-j$ and $k-j$ in a triplet $i-j-k$ close to initial value θ_{ijk} :

$$V_b = \frac{1}{2} k_b [\cos(\theta_{ijk}) - \cos(\theta_{0ijk})]^2 \quad (6)$$

where θ_{ijk} is the angle between the vectors $i-j$ and $k-j$ created by the joined particles and k_b is the bending constant.

The value of the angle θ_{ijk} can be obtained from:

$$\cos(\theta_{ijk}) = \frac{r_{ij}r_{kj}}{|r_{ij}||r_{kj}|} \quad (7)$$

Another configuration which was taken into account in the presented model is described by the torsion potential energy function Equation (8), which is applied to each $i-j-k-l$ quadruple in the aggregate's structure, Figure 1 (c). Equation (8) keeps the angle φ_{ijkl} between the normal vectors of the planes created by the triplets of particles $i-j-k$ and $j-k-l$ close to the value φ_{0ijkl} and it represents resistance to torsion of quadruple configuration:

$$V_t(\varphi_{ijkl}) = \frac{1}{2}k_t[\cos(\varphi_{ijkl}) - \cos(\varphi_{0ijkl})]^2 \quad (8)$$

where k_t is the torsion constant, φ_{ijkl} is the angle created between the normal vector of the triplet $i-j-k$ particles and the normal vector created from the triplet $j-k-l$.

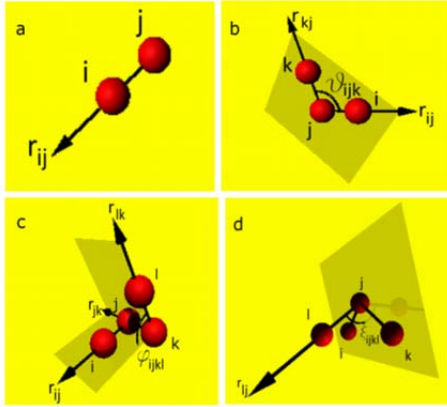


Figure 1: Various configurations of the connected particles in the fractal aggregates. The vectors referring to the connected particles were extended to find them easily. The spherical particles were minimised and joined by lines.

The angle φ_{ijkl} can be established from:

$$\cos(\varphi_{ijkl}) = \frac{\mathbf{A} \cdot \mathbf{B}}{|\mathbf{A}||\mathbf{B}|} \quad (9)$$

Normal vectors \mathbf{A} and \mathbf{B} of the planes created by the vectors of the $i-j-k$ and the $j-k-l$ particle configurations, respectively, are obtained from:

$$\mathbf{A} = r_{ij} \times r_{jk} \quad (10)$$

$$\mathbf{B} = r_{lk} \times r_{jk} \quad (11)$$

The last configuration of the particles can be modelled by the inversion potential energy, Equation (12). This potential energy function prevents this configuration of primary particles, depicted on Figure 1 (d) from inverting into its mirror configuration:

$$V_p(\xi_{ijkl}) = \frac{1}{2}k_p[\cos(\xi_{ijkl}) - \cos(\xi_{0ijkl})]^2 \quad (12)$$

where k_p is the inversion constant, ξ_{ijkl} is the angle between the plane created by the triplet of particles $i-j-k$ and the vector created by the particles $j-l$; Angle ξ_{ijkl} can be established following Equation (13), using normal vector \mathbf{A} of the plane created by the triplet of particles $i-j-k$ from Equation (10):

$$\sin(\xi_{ijkl}) = \frac{\mathbf{A} \cdot r_{lj}}{|\mathbf{A}||r_{lj}|} \quad (13)$$

In the same quadruple configuration, Figure 1 (d), one can observe two more angles: the angle between vector $k-j$ and the plane $i-j-l$ and the angle between the vector $i-j$ and the plane $k-j-l$. Therefore, the inversion potential energy function involves three angles in the same configuration of four particles. Note that the central particle j can have up to several neighbouring particles.

3. Equation of motion

Determining the motion of an aggregate is still complex and unsolved mathematical problem. Nevertheless, the evolution of the aggregate structure can be followed by calculating the motion equations for each constituent spherical particle of the ensemble. Conveniently, Equation (14) represents a sum of all of the forces contributing to the movement of the i -th particle in the aggregate in the single time step. To obtain the positions of the N particles of the aggregate in three-dimensional space, the system of N -number of equations must be solved for each constituent particle using Verlet's algorithm (1961). During the simulation process of the aggregate interaction forces between connected primary are calculated in each time step.

$$m_{pi} \frac{dv_i}{dt} = \sum_{i=1}^n \mathbf{F}_i^s - f_d \mathbf{v}_i + \sum_{i=1}^n \mathbf{F}_i^b + \sum_{i=1}^n \mathbf{F}_i^t + \sum_{i=1}^n \mathbf{F}_i^p + \mathbf{F}_i^D \quad (14)$$

where \mathbf{v}_i is the velocity of the particle in the aggregate and \mathbf{F}^s , \mathbf{F}^b , \mathbf{F}^t and \mathbf{F}^D are bond, bend, torsion, inverse and drag forces, respectively. To ensure the accuracy and control stability of the numerical simulation, all equations of motion were integrated using a very small time step, $\Delta t = 1 \cdot 10^{-11}$ s. The drag force acting on i -th particle under creeping flow condition can be obtained using following equation:

$$\mathbf{F}_i^D = -3\pi\mu d_p \frac{f_i}{C_s} (\mathbf{U} - \mathbf{v}_i) \quad (15)$$

where C_s is the Cunningham slip correction factor and \mathbf{U} is fluid velocity vector. Drag force has been calculated with the included hydrodynamic correction factor, f_i (Moskal and Payatakes, 2006). Equation (16) gives the value of the hydrodynamic factor for the i -th particle, taking into account the number of the neighboring particles of the i -th particle in the aggregate, which in result giving a lower value of drag force compared to the value taken from Stokes formula for single particle:

$$f_i = 1 - 0.871 \left(\frac{n_i}{27} \right)^{0.375} \quad (16)$$

where n_i is the number of neighbor particles of i -th particle in aggregate.

4. Results and discussion

Numerical simulation conducted here used aggregates with different sizes and fractal dimensions. Aggregates, one at the time, are placed on the rigid surface in the center of rectangular tunnel with open upper part, Figure 2 (left), and subjected to the linear flow profile, Figure 2 (right). Each aggregate was rotated before the movement in order to gain different orientation relatively to the flow direction. Aggregate are assumed to move horizontally along with the direction of the airflow and structure bounces up, when rigid surface is touched by any of the spherical primary particles of aggregate. Diffusion Limited Aggregation algorithm (Witten and Sander, 1981) was used to generate aggregates with fractal dimensions $D_f=1.6, 1.8$ and 2.2 and the number of primary particles $N=20$ and 40 .

Depending on the fractal dimension of the structure, lift-off from the surface can be detected after different time interval. Here, we monitor center of the mass which describes the aggregate structure final position after specified time interval, $\Delta t_{int} = 1 \cdot 10^{-5}$ s. We calculate the ratio between location of the center of the mass after certain time interval to location of the initial center of the mass, y/y_0 for each aggregate. This allow us to judge the structure's ability to lift-off. The final altitude of the center of the mass of aggregate was achieved for $\Delta t < \Delta t_{int}$. Parameters which were used in the simulation are shown in Table 1. The values of the air flow allow us to neglect the Brownian force. The disturbance of the neighboring primary particles are taken into account to obtain value of the hydrodynamic drag force acting on each constitutive particle in aggregate.

4.1. Lift –off of the aggregates with deformable structure

As the numerical results indicate using deformable model, aggregates with more open morphology are lifted-off easier than aggregates with compacted structure. This can be seen by comparing the final value of y/y_0 of aggregate after imposed time interval in the simulation Figure 3 (left). One may expect that the reason why more open aggregates reach equilibrium point at greater y/y_0 value is connected strongly with their morphology. This can be seen for aggregates with $N=40$. Results are not consistent for aggregates with $N=20$ (case 3), Figure 3. This can be explained by the fact that aggregates composed of number of primary particles below $N < 20$ do not obey fractal like geometry (Moskal and Payatakes, 2006). Comparing the same aggregates when altering the flexibility, Figure 3, one can see that aggregates do not exhibit the huge differences in terms of the final y/y_0 value. However the aggregates which are less flexible (case1) are lifted higher.

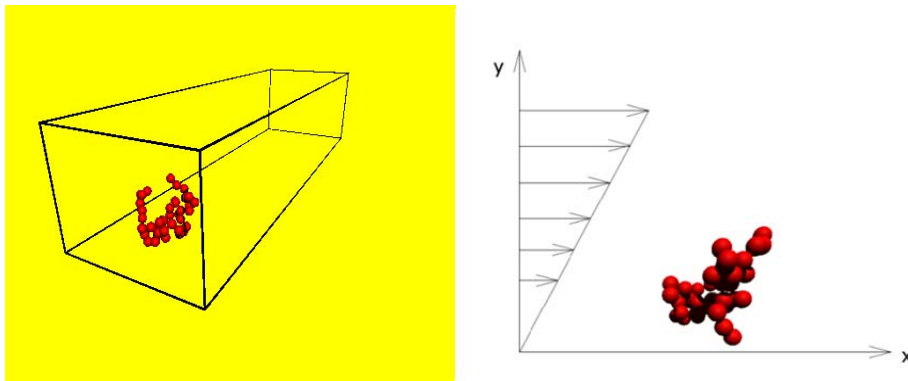


Figure 2: Rectangular tunnel as the control volume of the experiment (left), Aggregate structure under the shear flow in the tunnel (right)

Table 1: Parameters used in the simulations.

Symbol	Case 1	Case 2	Case 3
N	40	40	20
E [Pa]	$4 \cdot 10^{10}$	$2 \cdot 10^{10}$	$4 \cdot 10^{10}$
g [J m^{-2}]	0.15	0.08	0.15
ν	0.27	0.20	0.27
k_s [kg s^{-2}]	100	50	100
k_b [kg m s^{-2}]	10^{-22}	10^{-25}	10^{-22}
k_t [kg m s^{-2}]	10^{-22}	10^{-22}	10^{-22}
k_p [kg m s^{-2}]	10^{-22}	10^{-22}	10^{-22}

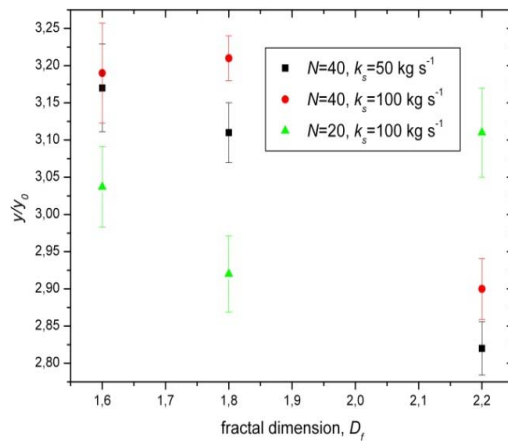


Figure 3: Value of the center of the mass relative to the initial value of the center of the mass (y/y_0 'coordinate) for aggregates with different D_f and N

4.2. Deformable aggregates vs. rigid body aggregates

As the simulation results indicate, without any doubt, deformation of the aggregate's structure influence the final y/y_0 value. Interaction forces between primary particles in flexible aggregate model are contributing to the final position of the aggregate. Comparing the final value of y/y_0 between two models, one can see that aggregates with rigid structure can be hardly lifted, Figure 4.

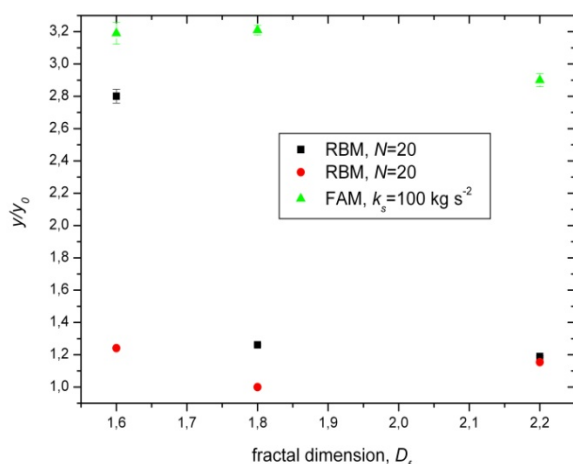


Figure 4: Compared results for aggregates with deformable structure (FAM) and rigid body (RBM).

5. Conclusions

Aggregates lift off phenomenon was investigated in this study using deformable aggregate model and the rigid body model. Both models were compared. Results clearly indicate that lift-off of the structure depends on the fractal dimension of aggregate, number of constitutive particles and deformability of the structure. For stiff aggregates investigated by the rigid body model, aggregates are hardly lifted by the flow of the air for any fractal dimension.

Acknowledgments

This work was supported by National Science Centre, Poland under Grant number UMO 2015/19/B/ST8/0599

References

- Brasil, A.M., Farias, T.L., Carvalho, M.G., Koylu, U.O., 2001, Numerical characterization of the morphology of aggregated particles. *Journal of Aerosol Science*, 32, 489-508.
- Gac, J., Sosnowski, T.R., Gradoń, L., 2008, Turbulent flow energy for aerosolization of powder particles. *Journal of Aerosol Science*, 39, 113-126.
- Gradoń, L., 2009, Resuspension of particles from surfaces: Technological, environmental and pharmaceutical aspects. *Advanced Powder Technology*, 20, 17-28.
- Grzybowski, K., Gradoń, L., 2005, Modeling of the re-entrainment of particles from powder structures. *Advanced Powder Technology*, 16, 105-121.
- Moskal, A., Payatakes, A.C., 2006, Estimation of the diffusion coefficient of aerosol particle aggregates using Brownian simulation in the continuum regime. *Journal of Aerosol Science*, 37, 1081-1101.
- Przekop, R., Grzybowski, K., Gradoń, L., 2004, Energy-Balanced oscillatory model for description of particles deposition and re-entrainment on fiber collector. *Aerosol Science and Technology*, 38, 330-337.
- Reeks, M.W., Reed, J., Hall, D., 1988, On the resuspension of small particles by turbulent flow, *Journal of Physics D*, 21, 574-589.
- Reeks, M.W., Hall, D., 2001, Kinetic models for particle resuspension in turbulent flows: theory and measurement. *Journal of Aerosol Science*, 32, 1-31.
- Telko, H.J., Hickey, A.J., 2005, Dry Powder Inhalers Formulation, *Respiratory Care*, 50, 1209-1227.
- Verlet, L., 1961, Computer "Experiments" on Classical Fluids. I. Thermodynamical Properties of Lennard-Jones Molecules. *Physical Review*, 159, 98-103.
- Witten, Jr., T.A., Sander, L.M., 1981, Diffusion-Limited Aggregation, a Kinetic Critical Phenomenon. *Physical Review Letters*, 47, 1400-1403.
- Ziskind, G., Fichman, M., Gutfinger, C., 2000, Particle behavior on surfaces subjected to external excitations. *Journal of Aerosol Science*, 31, 703-719.